

Supporting Information

Inter-particle DNA walker amplification coupled with target self-convert for sensitive detection of multiple miRNA by liquid chromatography

Daxiu Li,^{a*} Yuhao Li,^a Yao Qin,^b Yike Tang,^a Xin Xie,^a Tingting He,^a Jian Tian,^a Kai Shi^{c*}

^aChongqing Key Laboratory of Target-Based Drug Discovery and Research, College of Pharmacy and Biological Engineering, Chongqing University of Technology, Chongqing 400054, PR China

^bChongqing Academy of Metrology and Quality Inspection, Chongqing 401120, PR China

^cCollege of New Energy Materials and Chemistry, Leshan Normal University, Leshan, Sichuan, 614000, PR China

Content

S1. Chemicals and apparatus	S2
S2. Coupling efficiency between MBs and DNA probes	S2
S3. Size Characterization and Zeta potential of MB-DNA probe	S3
S4. Optimization of Instrument Conditions	S3
S5. Reproducibility of the method	S3
S6. Supplementary Figures	S4
Figure S1 The peak area of S1/S2/S3 solutions before and after combing with MBs.	
Figure S2 Influence of mobile phase ratio on the signal intensity.	
Figure S3 Influence of column temperature on the signal intensity.	
Figure S4 Reproducibility of this method.	
S7. Supplementary Tables	S6
Table S1 Sequence information of probes used in the work	

S1. Chemicals and apparatus

All HPLC-purified oligonucleotides used in this study were purchased from Sangon Biotech (Shanghai, China) and list in Table S1. The streptavidin-modified magnetic beads (1 μm ; biotin binding capacity) were purchased from Aladdin Co. Ltd (Shanghai, China). The phosphate buffer saline (PBS, pH 7.4) contained 137 mM NaCl, 2.7 mM KCl, 1.5 mM KH_2PO_4 and 8 mM K_2HPO_4 . Tris-HCl buffer (pH 6.8) contain 20 mM Tris-HCl and 137 mM NaCl. NH_4Ac buffer (pH 6.8) contain 500 mM $\text{CH}_3\text{COONH}_4$. 1,1,1,3,3,3-Hexafluoro-2-propanol (HFIP) were supplied by Macklin Biochemical Co., Ltd (Shanghai China). Ethylenediamine tetraacetic acid disodium salt (Na_2EDTA), MgCl_2 and other used chemicals were procured from Abcam Co. Ltd (Shanghai, China). All solutions used in the experiments were prepared with ultrapure water, exhibiting a specific resistance of $18.25 \text{ M}\Omega\cdot\text{cm}^{-1}$.

HPLC analysis was performed using a Shimadzu 20-AD system coupled with an SPD-M20A photodiode array detector. Separation of the analytes was achieved on a Phenomenex Clarity Oligo-MS column (Torrance, CA, USA) with dimensions of 100 mm \times 4.6 mm internal diameter and a particle size of 2.6 μm . The mobile phase A consisted of 100 mM HFIP and 4 mM TEA in 2% methanol. The mobile phase B formed by 100 mM HFIP and 4 mM TEA in 98% methanol. The column temperature was fixed constant at 40 $^\circ\text{C}$. The proportion of mobile phase B was linearly increased from 5% to 20% over a period of 10 minutes at a flow rate of 1.0 mL/min. After that, it holds for 10 minutes for the elution of probes, the wavelength was set at 260 nm.

S2. Coupling efficiency between MBs and DNA probes

To explore the coupling efficiency of MBs and DNA probes, the peak area of DNA probes was measured by HPLC before and after conjugation by taking S1/S2/S3 in MB2 as an example. As shown in Fig. S1, the peak area of S1/S2/S3 were measured before and after conjugation. The area reduced 32.1%, 30.5% and 31.7% responding to S1/S2/S3, respectively, indicating the successful coupling of MBs and S1/S2/S3.

S3. Size Characterization and Zeta potential of MB-DNA probe

40 μL 1 $\text{mg}\cdot\text{mL}^{-1}$ MB-DNA was diluted in 2 mL Tris-HCl buffer. 5 μL of 10 $\text{mg}\cdot\text{mL}^{-1}$ MB were dispersed in 2.5 mL of Tris-HCl buffer, ensuring the concentration of the MB-DNA probes was the same as the concentration of the single MB. Finally, the size and Zeta potential of the MB-DNA and MBs were determined by nanoparticle size and surface potential analyzer, indicating the successful coupling of MBs and DNA probes.

S4. Optimization of Instrument Conditions

Typically, the mobile phase ratio and column temperature in the elution procedure were optimized. In the liquid chromatographic analysis process, higher organic phase ratios and column temperatures have significant effects on the performance of separation. Reasonable ratio and temperature can reduce column pressure and improve peak shape and column efficiency greatly. However, excessive organic phase or higher column temperatures may lead to insufficient or premature elution of the analyte and poor peak shape. Thus, it was extremely vital to select an appropriate mobile phase ratio and column temperature for target detection. Fig. S2 and Fig. S3 revealed that peak patterns changed with variation of organic phase ratio and temperature. The proportion of mobile phase B at 20% and column temperature at 40 $^{\circ}\text{C}$ presented better peak shapes. Therefore, the optimal mobile phase ratio and column temperature were 20% and 40 $^{\circ}\text{C}$.

S5. Reproducibility of the method

In order to demonstrate the reproducibility of this proposed method, three parallel experiments were prepared with similar operation and peak areas were investigated through the detection of 1 pM miRNA-21/199a/499. As can be seen from Fig. S4, the similar areas were obtained of three parallel experiments in blank group and target group, indicating a great reproducibility of this method. The relative standard deviation (RSD) of the peak area of miRNA-21/199a/499 system in target groups were 4.59%, 4.54% and 2.67%, respectively.

S5. Supplementary Figures

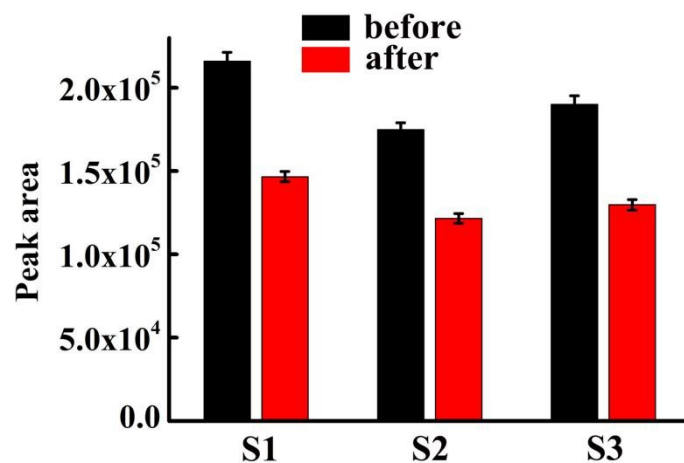


Fig. S1 The peak area of S1/S2/S3 solutions before and after combining with MBs. Error bars: SD; n = 3.

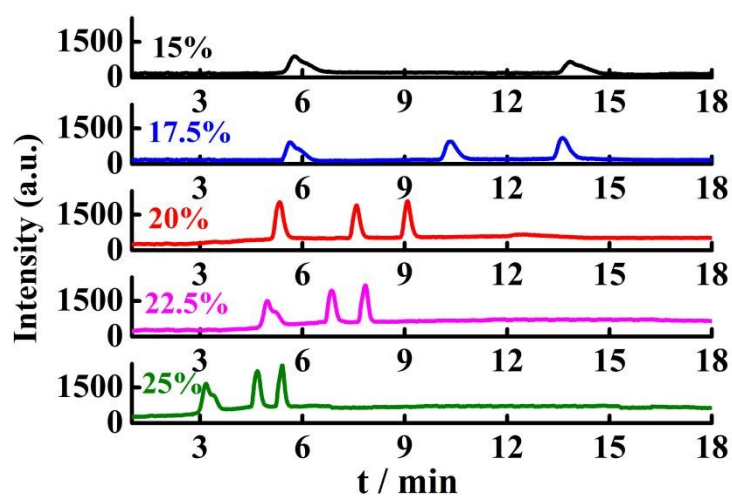


Fig. S2 Influence of mobile phase ratio on the signal intensity.

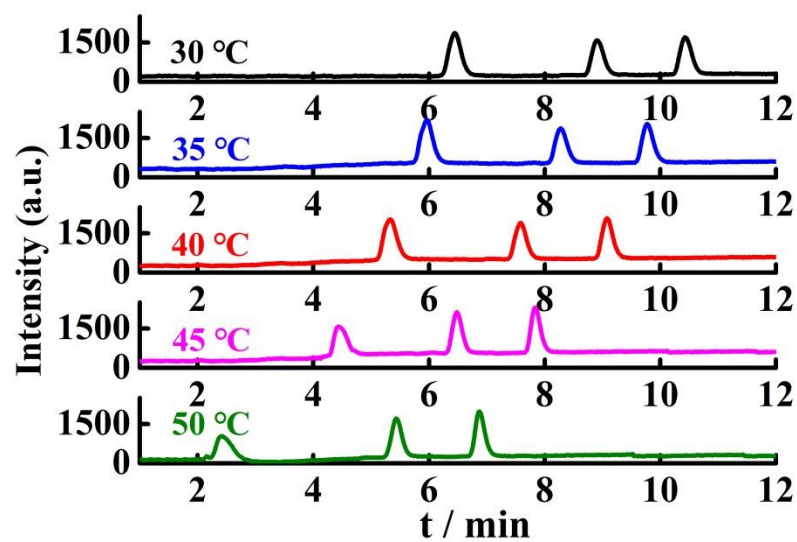


Fig. S3 Influence of column temperature on the signal intensity.

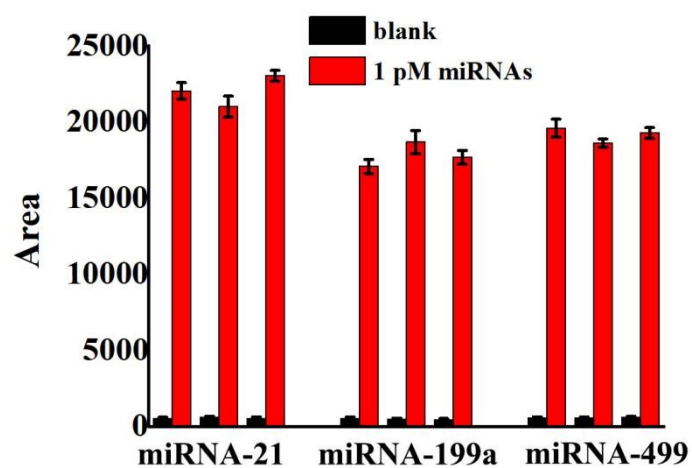


Fig. S4 Reproducibility of this method. Error bars: standard deviations of three parallel experiments.

S7. Supplementary Tables

Table S1. Sequence information of probes used in the work

Name	Sequence (5'-3')
miRNA-21	5'-UAGCUUAUCAGACUGAUGUUGA-3'
miRNA-199a	5'-CCCAGUGUUCAGACUACCUGUUC-3'
miRNA-499	5'-UUAAGACUUGCAGUGAUGUUU-3'
H1-21	5'-AAAAAAAG GCGATT <u>CAACAT</u> CAGTCTGATAAGCTATGTT GACACCCATGTAGCTTATCAGACTGAAAAAA-biotin-3'
H1-199a	5'-AAAAAAG AGCGAT <u>GAACAG</u> GTAGTCTGAACACTGGGCT GTTCCACCCATGCCAGTGTTCAGACTAAAAAA-biotin-3'
H1-499	5'-AAAAAAG AGCGAT <u>AAACAT</u> CACTGCAAGTCTTAAATGT TTCACCCATGTTAAGACTTGCAGTGTATAA-biotin-3'
H2-21	5'-AAGCTACATGGGTGTCAACATAGCTTATCAGACTGATGT TGACACCCAT GTT CTCAGGC-3'
H2-199a	5'-ACTGGGCATGGGTGGAACAGCCCAGTGTTCAGACTACCT GTTCCACCCAT GTT GCATCACT-3'
H2-499	5'-TCTTAACATGGGTGAAACATTTAAGACTTGCAGTGTATGT TTCACCCAT GTT ATGATGTC-3'
S-1	5'-biotin-TTTTTGCCTGAGT r ACTTTTTTTTTTTT-3'
S-2	5'-biotin-TTTTTAGTGATGCT r ACTTTTTTTTTTTTTT-3'
S-3	5'-biotin-TTTTTGACATCATG r ACTTTTTTTTTTTTTTTTTT-3'
miRNA21-M1	5'-UAGCUAAUCAGACUGAUGUUGA-3
miRNA-199a-M1	5'-CCCAGUAUUCAGACUACCUGUUC-3'
miRNA-499-M1	5'-UUAAGAAUUGCAGUGAUGUUU-3'
miRNA21-M2	5'-UAGCUAAUCAGACUGGUGUUGA-3
miRNA-199a-M2	5'-CCCAGUAUUCAGACUGCCUGUUC-3'
miRNA-499-M2	5'-UUAAGAAUUGCAGUGGUGUUU-3'
miRNA21-NM	5'-GCAUCGGAAGCGAGAGUUGGCU-3'
miRNA-199a-NM	5'-UGGCCAUAGGUUCGAGGACACCG-3'
miRNA-499-NM	5'-GCGGAUGAGCUCAACCGAGGC-3'
miRNA-21	5'-UAGCUUAUCAGACUGAUGUUGA-3'
miRNA-199a	5'-CCCAGUGUUCAGACUACCUGUUC-3'
miRNA-499	5'-UUAAGACUUGCAGUGAUGUUU-3'

Bold sequence: DNAzyme; underlined sequence: toehold region; red sequence: mismatch bases.